Journal of Labelled Compounds and Radiopharmaceuticals

Published online 11 May 2010 in Wiley Interscience (www.interscience.wiley.com) DOI: 10.1002/jlcr.1763

10th International Symposium on the Synthesis and Applications of Isotopes and Isotopically Labelled Compounds—Whole-Body Autoradiography (WBA)-Drug Discovery and Development

Session 3: Monday, June 15, 2009

SESSION CHAIRS: BRIAN WHITBY[a] and ALFRED LORDI[b]

[a]Covance Laboratories, Europe
[b]QPS, LLC, USA

Abstract: The use of QWBA and MARG in studying tissue distribution of receptor binding proteins was discussed.

Keywords: Erythropoietin receptor; Dosimetry; Quantitative Whole-Body Autoradiography (QWBA); Microautoradiography (MARG)

TISSUE DISTRIBUTION OF A ERYTHROPOIETIN RECEPTOR BINDING PEPTIDE IN RATS SHOWN BY QUANTITATIVE WHOLE-BODY AUTORADIOGRAPHY (QWBA) AND MICROAUTORADIOGRAPHY (MARG)

ERIC SOLON[a], KATHRYN W. WOODBURN[b], PAUL STRZEMIENSKI[a], QING FAN[b], CAIDING XU[b] AND CHRISTOPHER P HOLMES[b]

[a]QPS, Newark, DE, USA
[b]Affymax Inc, Palo Alto, CA, USA

Abstract: The tissue distribution of a peptide related to a family having erythropoiesis stimulating activity, binds to erythropoietin receptor (EPOr), but has no sequence homology to the human EPOr, was evaluated in albino rats given a single intravenous (IV) or a subcutaneous (SC) dose of the ^{14}C-Test Peptide at 5 mg/kg. Rats were euthanized at 1, 4, 8, 24, 72, 120, 168, 336, and 672 h post-dose (IV), or at 1, 24, and 168 h post-dose (SC). Tissue concentration and localization was demonstrated using QWBA and MARG. Drug-derived radioactivity was distributed to tissues of rats through 672 h and 168 h post-IV or SC dose, respectively. The highest concentrations of radioactivity found at 1 h post-dose were in the renal cortex and medulla, liver, blood vessels, spleen, and bone marrow. There was differential distribution between the red and white pulp of the spleen. Similar patterns of tissue distribution were observed following IV and SC administration. analysis of the kidney showed radioactivity localized to the glomeruli and tubules, which suggested a route of elimination of drug-derived radioactivity, and/or binding to renal EPOr. MARG results suggested that radioactivity partitioned into the liver, spleen, lymph nodes and thymus (extramedullary hematopoietic sites). MARG on bone marrow showed a very high localization, which was likely a function of the known high density of EPOr in the bone marrow. These data suggest that the Test peptide, which binds to the EPOr, but has no sequence homology to rHuEPO, localizes selectively to known erythropoietic tissues.

Keywords: Tissue Distribution; Erythropoietin Receptor; Quantitative Whole-Body Autoradiography, Microautoradiography

Introduction: Recombinant erythropoietin has been shown to successfully treat anemia in patients undergoing chemotherapy and those with chronic kidney disease[1]. Several pharmaceutical companies are developing agents to stimulate human erythropoiesis in an effort to treat this type of anemia. The tissue distribution and positive identification of the EPO receptor (EPOr) is not well understood. The objective of this study was to evaluate the tissue distribution of a ^{14}C-labeled Test Peptide related to a peptide family having erythropoiesis stimulating activity, and that binds to EPOr, but has no sequence homology to the human EPO receptor.

Methods: Dose Preparation: The test article peptide (M.W. 4877, free base) was radiolabeled by GE Healthcare (Buckinghamshire, UK). The dosing formulation was prepared by solubilizing [^{14}C]Test Peptide in 10 mM acetate buffered saline. The same formulation

Table 1. Study Design and Animal Treatments

Group Number	Number/Strain/Sex	Dose Route	Dose Form[a]	Compound AF37092 & Target Dose Level (mg/kg)	Target Dose Volume (mL/kg)	Target Dose Concentration (mg/mL)	Target Radioactivity Level (μCi/kg)
1	9/Sprague Dawley/Male[b]	IV	Solution	5	2	2.5	106.5
2	3/Sprague Dawley/Male[c]	SC	Solution	5	2	2.5	106.5
3	3/Sprague Dawley/Male[d]	IV	Solution	5	2	2.5	106.5

[a]IV and SC Dose solution prepared in acetate buffered saline, pH 5–6.
[b]Group 1: One rat per group per time point will be euthanized at 1, 4, 8, 24, 72, 120, 168, 336 and 672 h post-dose for QWBA and blood collection.
[c]Group 2: One rat per group per time point will be euthanized at 1, 24, and 168 h post-dose for QWBA and blood collection.
[d]One rat per time point will be euthanized at 1, 24, and 168 h post-dose for tissue collection: kidney, spleen, femur (bone marrow), lymph nodes, thymus, and liver.

was used for both IV and SC dose administration. The formulation was determined to be homogeneous and the test article had a radiopurity of $>97\%$. The specific activity of [^{14}C]Test Peptide in the dosing formulations was determined to be 22.77 μCi/mg of free test article.

Animal Experimentation: All rats were maintained in an AAALAC International Approved animal facility. The study design and animal treatments are outlined in Table 1.

Quantitative Whole-Body Autoradiography Analysis: Standard validated QWBA methods [2] were used and are briefly described as follows. Blood was collected via cardiac puncture for blood and plasma LSC analysis immediately before being euthanized by submersion in a hexane/dry ice bath. (15 min freeze time). Carcasses were freeze-embedded in a 2% carboxymethylcellulose. 40 μm thick sections collected using a Leica CM3600 Cryomacrocut, maintained at approximately -20°C. Dehydrated sections were co-exposed with ^{14}C Blood calibration standards, to Fuji Imaging plates for 4 days. Images obtained using a Typhoon 9410 Phosphor Imager. Tissue concentrations determined by image analysis conducted using MCID Elite Image Analysis system. The lower limit of quantitation (LLOQ) and upper limit of quantitation (ULOQ) were based on the lowest (0.00084264 μCi/g) and highest (8.177 μCi/g) standards used in the calibration curve. For this study the LLOQ was 0.037 μg equiv/g of tissue and the ULOQ was 359.113 μg equiv/g of tissue.

Microautoradiography Analysis: Microautoradiography was based on the methods of Stumpf [3] and Appleton [4], and are briefly described as follows. Group 3 animals were deeply anesthetized with isoflurane and euthanized by whole-body perfusion with 50–100 mL of saline. Bone marrow, kidney, liver, lymph nodes, spleen, and thymus were removed and snap-frozen in Nliq. Samples were cryosectioned (5 μm thick) at approximately -18°C under darkroom conditions, and sections were thaw-mounted onto slides previously coated with nuclear photographic emulsion. Slides were placed into black light-tight slide boxes containing dessicant and incubated at 4°C for 7 days. Some slides were exposed longer to confirm possible changes in radioactive distribution. Slides were developed in Kodak D19 developer, rinsed in water, fixed, rinsed in water again, and stained with hematoxylin and eosin. The slides were dehydrated with an alcohol gradient, cleared in xylene and permanently mounted.

Results and Discussion: Tissue Distribution by QWBA and LSC: Whole-body autoradiograms showing patterns of radioactivity distribution in tissues are illustrated in Figure 1. Concentrations of drug-derived radioactivity in the tissues of rats following IV or SC bolus administration of [^{14}C]Test Peptide are summarized in Table 2. Drug-derived radioactivity was widely distributed to tissues of male Sprague-Dawley rats through 672 h and 168 h post-IV or -SC dose. The highest concentrations of radioactivity found at 1 h post-IV dose were in the renal cortex and medulla, liver, blood vessels, spleen, and bone marrow. Concentrations in the blood vessels remained relatively high throughout the duration of the study. There was a marked difference in tissue concentrations found between the red pulp and white pulp in the spleen. The tissue kinetics reflected a more gradual distribution of radioactivity over time following SC administration compared to an IV administration. Tissue concentrations of radioactivity were typically greater following IV dosing compared to SC administration. The blood & plasma data suggested that the test article was retained in the cellular portions of blood. Elimination was incomplete at 672 h post-dose.

Microautoradiography (MARG): Microautoradiographs are not shown. Radioactivity in kidney localized to glomerulii, tubules and associated ducts, which suggested excretion of drug-derived radioactivity and/or or binding of the radioactive moiety to renal EPO receptors. Radioactivity in liver samples localized to discrete cellular aspects, which were believed to be hepatocytes and sinusoidal spaces. Radioactivity in spleen showed a substantial difference in the distribution between white and red pulp, which were consistent with QWBA results. The red pulp is a site of extramedullary hematopoiesis. Thymus showed radioactivity diffusely distributed at a low density up to 24 h, but was localized at discrete locations (trabecular regions and reticular cells) at 168 h post-dose. Lymph nodes showed relatively low levels of radioactivity that appeared to be evenly distributed throughout the tissue. Radioactivity appeared to partition into lymph nodes where it remained longer than in the blood. Bone marrow showed very dense localization of radioactivity after a relatively short development time (1 day), which made evaluation difficult. Due to the density of localization, and sectioning difficulty, no discernable cellular morphology could be identified. It is likely that the radioactivity density reflected binding to the high density of EPO receptors.

Journal of
Labelled Compounds and
Radiopharmaceuticals

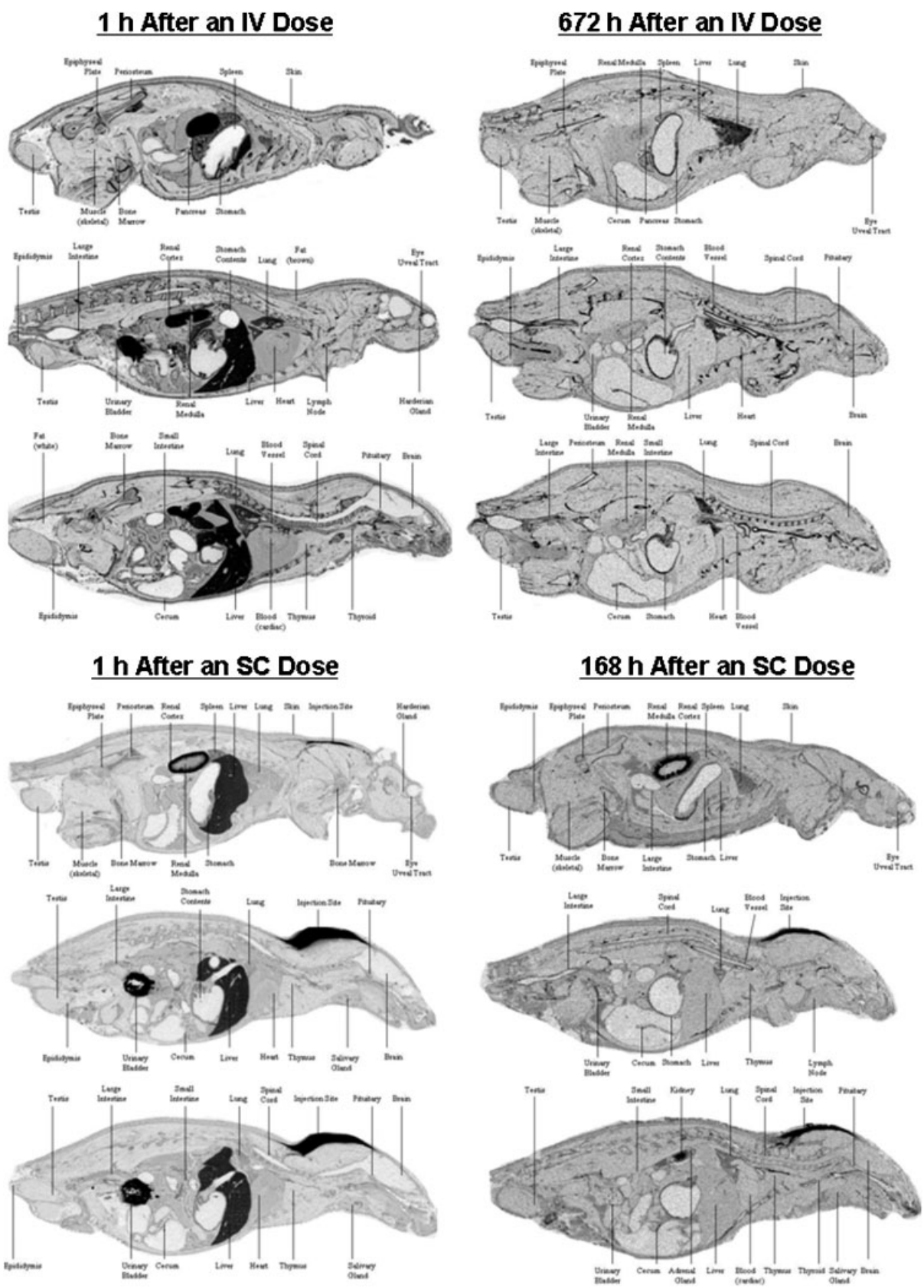

Figure 1. Whole-Body Autoradioluminographs of Rats given a Single IV or SC Administration of [^{14}C]Test Peptide.

Journal of Labelled Compounds and Radiopharmaceuticals

Table 2. Concentrations of radioactivity in tissues of male Sprague–Dawley rats After a single IV or SC dose of [^{14}C]test peptide at 5 mg/kg

Tissue type	Tissue	Mean - µg equiv/g tissue											
		IV									SC		
		1 h	4 h	8 h	24 h	72 h	120 h	168 h	336 h	672 h	1 h	24 h	168 h
Vascular/Lymphatic	Blood (cardiac)	1.692	1.386	0.481	0.308	0.141	0.121	0.069	0.075	0.039	0.960	0.292	0.092
	Blood (LSC)	1.661	0.706	0.462	0.256	0.139	0.098	0.067	0.070	0.043	0.708	0.218	0.087
	Plasma (LSC)	2.436	1.048	0.711	0.304	0.107	0.053	0.023	BQL	BQL	1.070	0.255	0.025
	Blood vessel	17.529	17.934	17.129	10.197	10.418	10.624	7.245	7.795	8.880	6.622	4.556	2.437
	Bone marrow (femur)	5.230	2.604	2.231	0.559	0.274	0.174	0.116	0.058	BQL	2.620	0.999	0.164
	Lymph node	1.054	1.819	1.710	0.941	0.462	0.582	0.222	0.145	0.134	1.016	2.072	0.527
	Spleen	9.064	5.311	4.839	1.682	0.638	0.404	0.192	0.193	0.234	3.489	1.363	0.205
	Thymus	1.140	0.841	0.649	0.461	0.304	0.182	0.118	0.058	0.040	0.352	0.561	0.155
Excretory/Metabolic	Bile (in duct)	NS	NS	NS	NS	NS	NS	NS	NS	NS	NS	NS	NS
	Kidney (renal cortex)	83.779	8.609	6.497	3.319	1.926	1.031	0.686	0.393	0.166	15.666	2.775	0.911
	Kidney (renal medulla)	18.134	3.901	3.336	3.118	1.538	0.951	0.891	0.472	0.226	2.095	4.955	1.829
	Liver	17.955	8.492	4.718	1.335	0.418	0.233	0.172	0.089	0.037	11.197	1.512	0.159
	Urinary bladder	95.474	51.846	4.776	7.158	1.231	1.171	0.898	0.402	0.187	26.722	19.712	1.016
	Urinary bladder (contents)	348.422	149.072	7.810	1.363	0.300	0.048	0.225	BQL	BQL	57.004	9.171	0.205
Central Nervous System	Brain (cerebrum)	0.169	0.233	0.118	0.116	0.101	0.114	0.081	0.095	0.055	0.067	0.126	0.083
	Brain (cerebellum)	0.243	0.278	0.144	0.138	0.132	0.124	0.106	0.104	0.060	0.078	0.169	0.108
	Brain (medulla)	0.148	0.233	0.138	0.131	0.125	0.132	0.091	0.086	0.070	0.049	0.152	0.101
	Spinal cord	0.203	0.340	0.202	0.152	0.145	0.205	0.152	0.107	0.104	0.084	0.176	0.166
	Meninges	2.389	NS	NS	NS	NS	NS	NS	NS	NS	NS	NS	NS
Endocrine	Adrenal gland	4.118	1.989	1.683	1.074	0.803	0.376	0.390	0.279	0.122	1.626	1.134	0.449
	Pituitary gland	3.180	2.889	0.882	0.847	0.361	0.332	0.190	0.119	0.173	0.778	0.558	0.243
	Thyroid	2.722	3.233	2.386	1.531	0.663	0.794	0.290	0.221	0.352	1.221	1.060	0.344
Secretory	Harderian gland	1.498	1.710	3.229	1.893	0.906	0.382	0.257	0.061	BQL	0.582	2.544	0.206
	Pancreas	2.110	1.785	1.251	0.723	0.389	0.306	0.136	0.133	0.061	0.752	0.683	0.200

	Salivary gland	2.207	1.997	2.032	0.782	0.309	0.285	0.187	0.086	0.040	0.698	0.616	0.219
Adipose	Adipose (brown)	1.700	2.217	1.374	1.210	0.675	0.575	0.306	0.151	0.110	0.478	1.697	0.363
	Adipose (white)	0.388	0.178	0.173	0.306	0.329	0.137	0.272	0.209	0.136	0.381	0.444	0.455
Dermal	Skin	2.481	2.551	3.244	1.673	0.994	0.629	0.321	0.319	0.261	0.925	1.129	0.308
Reproductive	Epididymis	2.474	1.878	1.321	1.121	0.326	0.566	0.215	0.100	0.107	0.597	0.373	0.168
	Prostate gland	3.086	1.812	1.458	1.697	0.589	0.301	0.502	0.185	0.169	0.497	1.026	0.139
	Seminal vesicles	1.813	1.505	2.227	1.186	0.657	0.478	0.330	0.114	0.158	0.327	0.854	0.267
	Testis	0.811	0.623	0.479	0.381	0.188	0.224	0.099	0.098	0.042	0.283	0.300	0.133
Skeletal/Muscular	Bone (femur)	0.668	0.503	0.497	0.185	0.146	0.238	0.551	0.379	0.120	0.526	0.364	0.052
	Bone (periosteum[a])	8.159	6.058	14.331	6.743	12.828	5.139	5.888	1.439	2.270	1.367	2.431	0.932
	Bone (epiphyseal plate)	17.505	8.448	7.244	2.819	1.567	1.033	2.074	1.949	0.612	2.161	1.614	0.327
	Heart	2.598	1.154	0.839	0.536	0.281	0.222	0.136	0.104	0.113	0.719	0.400	0.142
	Skeletal muscle	0.764	0.411	0.560	0.328	0.203	0.180	0.137	0.116	0.067	0.246	0.280	0.125
Respiratory	Lung	11.432	8.700	7.913	9.826	2.797	2.889	2.350	1.749	1.009	1.652	2.279	0.585
Alimentary Canal	Cecum	2.646	2.952	4.054	1.555	1.046	0.565	0.543	0.630	0.665	1.411	0.994	0.232
	Cecum (contents)	0.077	0.128	0.909	0.238	0.063	BQL	BQL	BQL	BQL	0.044	0.509	BQL
	Large intestine	6.045	10.081	3.451	3.992	3.202	1.240	0.785	0.553	0.704	1.744	2.236	0.417
	Lg. intestine (contents)	0.076	0.110	0.846	0.250	0.147	0.037	BQL	BQL	BQL	0.058	0.672	BQL
	Stomach	16.265	7.647	4.975	3.650	2.412	1.263	1.380	1.137	1.094	2.728	1.490	0.434
	Stomach (contents)	0.041	0.151	0.187	0.151	BQL	BQL	BQL	BQL	BQL	BQL	0.297	BQL
	Small intestine	2.171	2.602	2.455	1.076	1.222	0.761	0.421	0.304	0.261	2.344	1.484	0.266
	Sm. intestine (contents)	0.227	1.090	0.903	0.236	0.405	0.063	0.038	BQL	BQL	0.655	0.277	0.094
Ocular	Eye—lens	0.131	0.180	0.113	0.118	0.115	0.061	0.056	0.047	0.064	0.045	0.079	0.049
	Eye—uveal tract	6.747	3.723	2.753	1.302	1.053	1.042	0.665	0.241	0.315	0.628	0.983	0.218

NS = Not sampled, since not visualized on autoradioluminograph, considered as BQL; BQL = Value is below the LLOQ; LLOQ = 0.0008426 μCi/g/0.02277 μCi/μg = 0.037 μg equivalent/g tissue; ULOQ = 8.177 μCi/g/0.02277 μCi/μg equivalent/g tissue.

[a]Additional tissues sampled, since radioactive levels were present during image analysis.

J. Label Compd. Radiopharm **2010**, 53 269–274

www.jlcr.org

Journal of Labelled Compounds and Radiopharmaceuticals

Conclusions: In general, relative tissue radioactivity concentration profiles were similar at comparable time points following IV and SC administration. The tissue kinetics reflected a more gradual distribution of radioactivity over time following SC administration compared to IV administration. MARG results suggested that radioactivity partitioned into the liver, the spleen, the lymph nodes and thymus (extramedullary hematopoietic sites). MARG on bone marrow showed a very dense covering of exposed grains, which is likely a function of the high density of EPO receptors in the bone marrow. These data showed that this peptide which has no sequence homology to rHuEPO, localized selectively and in tissues that are believed to have EPOr. We are in the process of obtaining a specific antibody to confirm EPOr tissue distrubution and co-localization of the test article (^{14}C-Test Peptide) with the EPOr in MARG samples. Improvements made to the freezing procedure will also be applied in the next experiments to reduce artifacts.

References

[1] A. M. S. Belonje, R.A. de Boer, and A. A. Voors, *Cardiovasc Drugs Ther.* **2008**, 22, 1–2.
[2] E. Solon, *Expert Opin. Drug Discov*. **2007**, 2, 4, 503–514.
[3] W. E. Stumpf, *Drug Localization in Tissues and Cells*, IDDC Press, Library of Congress Control Number 2003105179, **2003**, pp. 32–51.
[4] T. C. Appleton, J. Royal Microscop. Soc., **1964**, 83, pp. 277–281.